PCCP

Accepted Manuscript

ROYAL SOCIETY OF CHEMISTRY

www.rsc.org/pccp

Journal Name

ARTICLE TYPE

Cite this: DOI: 10.1039/xxxxxxxxxx

Properties of noncovalent tetraphenylporphine···C_{60} dyad as studied by different long-range and dispersion-corrected DFT functionals

Oscar Amelines-Sarria,*[a] Vladimir A. Basiuk,[b] Víctor Duarte Alaniz[c] and Margarita Rivera[a]

Received Date
Accepted Date

DOI: 10.1039/xxxxxxxxxx

www.rsc.org/journalname

The noncovalent dyad of tetraphenylporphine and C_{60} fullerene (H_2TPP···C_{60}) and the tetraphenylporphine dimer (H_2TPP···H_2TPP) were studied by density functional theory (DFT), using functionals that incorporate empirical dispersion correction (DFT-D), functionals that use a long-range correction (LC) scheme, a hybrid functional (B3LYP) and a highly parametrized empirical exchange-correlation functional (M05-2X). The results were compared to X-ray structures and interaction energies reported in previous experimental and theoretical works. It was found that B3LYP and CAM-B3LYP functionals fail to reproduce the X-ray structures and binding energies of the TPP···C_{60} system. DFT-D functionals overestimated the $\pi\cdots\pi$ energy interactions for both systems, however, the optimized structures agree well with those observed experimentally. LC-BLYP functional predicts geometries similar to X-ray structures, nevertheless, due to the lack of correction in the dispersion energy, the predicted energies for both model systems are low. On the other hand, M05-2X functional exhibited the best performance. Both the structures and binding energies calculated with M05-2X are consistent with experimental and theoretical evidence reported by other authors, as well as with our experimental results obtained by means of atomic force microscopy on H_2TPP thin films grown on HOPG/C_{60} substrate by physical vapor deposition.

1 Introduction

Noncovalent interaction of fullerenes with porphyrins and their metal complexes have been extensively studied both experimentally and theoretically, primarily motivated by their importance for the applications in organic electron-optical devices for solar energy conversion technology, among others.[1–4] It was found experimentally that the fullerenes (C_{60} in particular) and substituted porphines based on meso-tetraphenylporphine (TPP), including their metal complexes, are capable of forming noncovalent complexes.[5–10] The main structural feature reported for these complexes is that the distance between C_{60} and porphyrins (2.6–3.0 Å) is unusually short compared to typical $\pi\cdots\pi$ interactions (3.0–3.5 Å). The short contact between TPP and C_{60} implies a considerable attractive interaction between the two molecules. Despite of a number of experimental reports, the nature of porphyrin–fullerene interaction is still not clearly understood, in particular aspects such as what type of interactions is responsible for the complex formation, the influence of central metal ion in the porphyrin on the interaction strength, *etc.*[11]

Quantum chemical calculations are an indispensable tool for the understanding of the nature of noncovalent porphyrins–fullerene interactions. Among the variety of computational methods, the density functional theory (DFT)[12] is the most convenient technique to study these and similar systems, due to its high cost–efficiency. The accuracy of DFT methods depends strongly on the approximation used for exchange-correlation energy functional (E_{xc}). The commonly used local density approximation (LDA) and generalized gradient approximation (GGA) functionals are purely local in nature, whereas in noncovalent systems the dispersion (attractive) and exchange (repulsive) interactions are nonlocal; as a result, LDA and GGA functionals fail to describe the long-range van der Waals (vdW) interactions. Thus, to describe noncovalent systems such as porphyrin–fullerene dyads more adequately, it is necessary to correct the above deficiencies.

One of the most widely employed and very well tested methods to include intermolecular dispersion interactions to DFT cal-

[a] *Instituto de Física, Universidad Nacional Autónoma de México, Sendero Bicipuma, Cd. Universitaria, C.P. 04510, Del. Coyoacán, Ciudad de México, México. E-mail: oscar.amelines@fisica.unam.mx*
[b] *Instituto de Ciencias Nucleares, Universidad Nacional Autónoma de México, Circuito Exterior s/n, Cd. Universitaria, C.P. 04510, Del. Coyoacán, Ciudad de México, México.*
[c] *Instituto de Química, Universidad Nacional Autónoma de México, Circuito Exterior, Cd. Universitaria, C.P. 04510, Del. Coyoacán, Ciudad de México, México.*

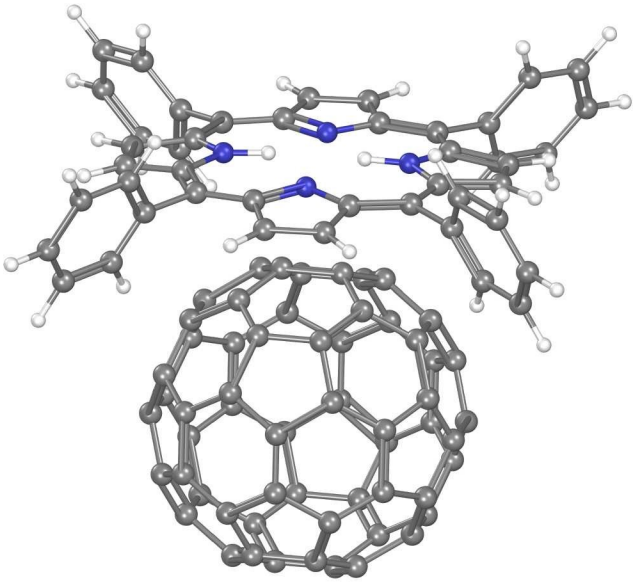

Fig. 1 Molecular structure of the $H_2TPP\cdots C_{60}$ complex.

culations, is referred to as DFT-D,[13–16] which introduces an additional empirical dispersion term to the conventional Kohn–Sham DFT energy. Here, the dispersion energy is simulated in the same way as in molecular mechanics, by adding a potential of the form C_6R^{-6} into the DFT energy, where R represents interatomic distances and C_6 are the dispersion coefficients. Meanwhile, the long-range corrected (LC) hybrid DFT schemes have been actively developed to correct the electron–electron exchange interaction in noncovalent systems.[17–20] The essence of the LC method is that the short-range exchange interaction is described by DFT, while for the long-range exchange interaction, 100 % HF exchange is used. Several authors emphasized that the inclusion of long-range exchange and dispersion interactions is crucial for a balanced representation of various types of weak interactions.[19,21]

A number of theoretical studies of $TPP\cdots C_{60}$ complexes have been carried out using pure DFT functionals,[6,22–26] and a few reports have employed dispersion-corrected computation schemes (DFT-D)[27–29] and hybrid functionals.[30] Table 1 summarizes some parameters obtained with DFT for $H_2TPP\cdots C_{60}$ dyad. The structure of $H_2TPP\cdots C_{60}$ complex is illustrated in Figure 1. Although it is well known that DFT results depend on the type of functional used, in Table 1 strong inconsistencies can be found despite of using the same functional and a similar basis set, which suggests that there are other parameters or interactions not considered in the model. For example, Boyd *et al.*[6] predicted for the $H_2TPP\cdots C_{60}$ complex a binding energy of -5.8 kcal mol^{-1} and a closer separation of 2.8 Å between porphyrin and fullerene calculated at the BLYP/DZP level of theory. At the same time, we found for the same complex an intermolecular separation of 4.0 Å and a repulsive interaction energy of 2.3 kcal mol^{-1} at a very similar level BLYP/DNP.[24] Wang *et al.*[22] found, for the same complex, a separation distance between porphyrin and C_{60} of 2.74 Å and a binding energy of -17.33 kcal mol^{-1} at the PBE/DZP level, while our calculation produced a value for binding energy of -2.2 kcal mol^{-1} and an intermolecular distance of 3.31 Å with a similar PBE/DNP level. We believe that all these inconsistencies and the fact that some authors report realistic results for optimized geometries (similar to the X-ray structures) are mainly due to fortuitous cancellation of errors, as suggested by other authors.[27] There are basically two errors involved in such cancellation: (i) the use of functionals unable to describe dispersion and exchange interactions at long distances, and (ii) the lack of correction (*e.g.*, by means of counterpoise correction, or CP[31]) for basis set superposition error (BSSE), which can cause an artificial shortening of intermolecular distances as well as artificial strengthening of intermolecular interactions in a noncovalent complex. It should be noted that unlike other authors, we consider the lack of correction to exchange interaction at long distances as one of the main erros in this calculations.

On the other hand, some publications employing DFT-D scheme to study $H_2TPP\cdots C_{60}$ complex, report porphyrin–fullerene distances close to those found in X-ray structures and large attractive binding energies (Table 1). Even though the above studies conclude that the contribution of dispersion interactions to the total binding energy is high, and although, these results are more reliable than those obtained with pure GGA and LDA functionals, none of them takes into account the real nature of vdW bonds. Besides the dispersion interaction, vdW bonds include long-range exchange interactions, which have not been taken into account in DFT calculations for $TPP\cdots C_{60}$ complexes until now.

As can be seen from this brief review, none of the DFT functionals used so far to study $H_2TPP\cdots C_{60}$ complex considered adequately long-range interactions present in the system. The main goal of our paper is to select a functional that describes more accurately the noncovalent interactions between porphyrin and fullerene, accounting for the balance of different forces in the system and a BSSE correction. In this sense, the long-range correction (LC) and dispersion-corrected DFT (DFT-D) scheme were tested. In addition, in order to take into account all weak interactions, a functional that incorporates both of the above schemes and a hybrid meta GGA functional were employed as well. In order to check the accuracy of our results, the calculated geometries are compared with experimental structures obtained by X-ray diffraction and with theoretical reports by other authors. In particular, the separation distance between porphyrin and fullerene based on the center of mass of both species, is obtained and compared with X-ray diffraction data. In order to test performance of the functionals used in this work, calculations of tetraphenylporphine–tetraphenylporphine ($H_2TPP\cdots H_2TPP$) dimer are also included. An additional information on the interactions in porphyrin–porphyrin and porphyrin–fullerene systems on a gas–solid interface was obtained from atomic force microscopy (AFM) observations of H_2TPP thin film at C_{60} layers previously deposited onto highly oriented pyrolytic graphite (HOPG) by vacuum sublimation.

Table 1 Separation distances (d_{cc} and $d_{C_{60}\cdots N}$, in Å) and binding energies (E_{bind} and E_{bind}^{CP}, in kcal mol^{-1}) reported for $H_2TPP\cdots C_{60}$ complex by using DFT with and without counterpoise (CP) correction for basis set superposition error (BSSE).

Functional/basis sets	d_{cc}[a]	$d_{C_{60}\cdots N}$[b]	E_{bind}	E_{bind}^{CP}	Ref.
BLYP/DZP	2.8	3.14	−5.8		6
BLYP/DNP	3.81	4.00	2.3		23,26
PBE/DZP	2.74		−17.33		22
PBE/DNP	3.31	3.53	−2.2		23,26
PBE/DZP	2.78		−18.22	−2.07	27
PBE/TZP	2.91		−2.07	0.92	27
B3LYP	3.1		−3.34		30
PBE/DZP+E_{disp}	2.44		−46.58	−24.90	27
PBE/TZP+E_{disp}	2.75		−22.37	−19.14	27
PBE-D3/def2-SVP	2.67		−27.0		28
PBE/DNP+E_{disp}	2.86	2.98	−25.5		29

[a] d_{cc} is the distance between the geometric centers of the porphyrin ring and the electron-rich 6:6 bond of the fullerene; [b] $d_{C_{60}\cdots N}$ represents the closest contacts of N atoms of tetraphenylporphine with 6:6 C−C bond of pyracylene unit of the C_{60}.

2 Methods and computational details

2.1 Computational details

For all electronic structure calculations, the Gaussian 09 software package was used.[32] The performance of six different functionals (B3LYP,[33] CAM-B3LYP,[34] LC-BLYP,[18] B97-D,[16] ωB97X-D[35] and M05-2X[36]) for the calculation of the $H_2TPP\cdots H_2TPP$ and $H_2TPP\cdots C_{60}$ systems have been tested. All the functionals were employed in conjunction with the 6-31G(d,p) basis set. Counterpoise correction was applied to all calculated binding energies in order to avoid the basis set superposition error.

B3LYP is a hybrid functional that combines the exchange-correlation of a conventional GGA method with a percentage of Hartree–Fock exchange (20 %). Due to this combination, B3LYP functional can describe exchange interaction to long distances. However, B3LYP fails to describe dispersion energy in a vdW complex because it uses correlation energy from GGA functionals, which are local in nature.

CAM-B3LYP and LC-BLYP functionals use the LC scheme. In the LC scheme[17,18] the two-electron operator $1/r_{12}$ is separated into short-range and long-range parts by using the standard error function, erf. In a short-range, the interaction is described by DFT exchange, while the long-range orbital-orbital exchange interaction is described with Hartree–Fock (HF) exchange integral, that is:

$$\frac{1}{r_{12}} = \underbrace{\frac{1-\mathrm{erf}(\mu r_{12})}{r_{12}}}_{SR} + \underbrace{\frac{\mathrm{erf}(\mu r_{12})}{r_{12}}}_{LR}, \qquad (1)$$

where μ is a parameter that determines the radio of each part.

B97-D uses the DFT-D method. Here, an empirical correction term is added to the DFT energy in order to take into account the dispersion interaction, such as:

$$E_{tot} = E_{DFT} + E_{disp}, \qquad (2)$$

where E_{disp} is an empirical dispersion correction.

ωB97X-D functional, which uses both LC and DFT-D schemes, is argued[35] to be generally superior in overall performance to pure LC, hybrid and other DFT-D functionals when calculating noncovalent energy interactions, equilibrium geometries, excited charge-transfer states and atomization energies.

In addition to the above, we analyzed the performance of one meta-GGA functional, namely M05-2X, on porphyrin–fullerene system. M05-2X is inferred to take into account "medium-range" electron correlations due to the way it is parametrized, which it is enough to describe the dispersion interactions in many complexes. Also, due to the high percentage of HF that M05-2X functional uses, the exchange interaction to long distance can be described by this functional.[36,37] The total energy is described by this functional as

$$E_{XC}^{hyb} = E_X^{HF} + \left(1 - \frac{X}{100}\right)(E_X^{DFT} - E_X^{HF}) + E_C^{DFT}, \qquad (3)$$

where E_X^{HF} is the Hartree–Fock exchange energy, E_X^{DFT} is the DFT exchange energy, and E_C^{DFT} is the DFT correlation energy. X, the percentage of Hartree–Fock exchange in the hybrid functional, is equal to 56, much higher than in B3LYP ($X_{B3LYP} = 20$). In this equation, the total correlation energy in DFT is modeled as the sum of the dynamic correlation energy given by E_C^{DFT} and the non-dynamical correlation energy contained in $\left(1 - \frac{X}{100}\right)(E_X^{DFT} - E_X^{HF})$.[36] As can be seen in Eq. 3, M05-2X has a different long-range exchange correction and medium-range dispersion energy correction compared to LC and DFT-D functionals, respectively.

2.2 Energy of interaction

The interaction energy between two molecules, which is useful and conceptually consistent, is given by the following expression:[38,39]

$$E_{int} = E_{AB}^{\alpha\cup\beta}(AB) - \left[E_A^{\alpha}(AB) + E_B^{\beta}(AB)\right], \qquad (4)$$

where $E_X^Z(Y)$ represents the energy of system X at geometry Y with a basis set Z. Eq. 4 is valid for any distance separation between the mass centers of the molecules. This definition is limited to the Born–Oppenheimer approximation for molecular

systems without considering relativistic effects and processes involving fast collisions. This is why, the definition is used in the *supermolecular approach* where energies are calculated in an approximated way for a given level of theory. It is important to emphasize that the energies of each monomer, E_A and E_B, are calculated using the dimer geometry, without any further optimization.[38,39]

When the supramolecular dimer is in a local minimum of the nuclear potential energy surface, the intermolecular energy interaction is called binding energy:

$$E_{\text{bind}} = E_{\text{int}}(AB)_{\text{eq}}. \quad (5)$$

Due to the finite size of the basis set used in such energy calculations, the values obtained are affected by BSSE, whose magnitude is comparable with that of the interaction energy. The BSSE error arises since E_A, and E_B quantities are calculated with a different basis size set in the supermolecular approach ($\alpha \cup \beta$) causing an additional artificial stabilization in E_{int} (Eq. 4).

The counterpoise method (CP)[31] can be used to correct this error. In CP procedure, the artificial stabilization energy for each monomer ($\delta_{AB}^{\text{BSSE}}$) is calculated and then added to the interaction energy obtained by using the supermolecular approach. For an AB dimer, the artificial stabilization energy, $\delta_{AB}^{\text{BSSE}}$ is:

$$\delta^{\text{BSSE}} = \left[E_A^{\alpha}(AB) - E_A^{\alpha\cup\beta}(AB)\right] + \left[E_B^{\beta}(AB) - E_B^{\alpha\cup\beta}(AB)\right]. \quad (6)$$

Including this quantity in Eq. 4 (in a local minima, $(AB)_{\text{eq}}$), the corrected binding energy ($E_{\text{bind}}^{\text{CP}}$) of a dimer takes the form of

$$E_{\text{bind}}^{\text{CP}}(AB) = E_{AB}^{\alpha\cup\beta}(AB)_{\text{eq}} - E_A^{\alpha}(AB)_{\text{eq}} - E_B^{\beta}(AB)_{\text{eq}} + \left[E_A^{\alpha}(AB)_{\text{eq}} - E_A^{\alpha\cup\beta}(AB)_{\text{eq}}\right] + \left[E_B^{\beta}(AB)_{\text{eq}} - E_B^{\alpha\cup\beta}(AB)_{\text{eq}}\right]. \quad (7)$$

After the cancellation of different terms in the previous equation, the following expression is obtained:

$$E_{\text{bind}}^{\text{CP}}(AB) = E_{AB}^{\alpha\cup\beta}(AB)_{\text{eq}} - \left[E_A^{\alpha\cup\beta}(AB)_{\text{eq}} + E_B^{\alpha\cup\beta}(AB)_{\text{eq}}\right]. \quad (8)$$

2.3 Experimental methodology

By using a physical vapor deposition (PVD) technique, a thin film of H_2TPP (TCI, Japan) was deposited onto a C_{60} (Sigma-Aldrich Company, USA, 99.5 %) film previously grown onto HOPG substrate to produce a multilayer HOPG/C_{60}/H_2TPP system. The pressure in the vacuum chamber before the film deposition was 10^{-6} Torr. In order to obtain experimental data complementing our results of DFT calculations, the surface of multilayer system was analyzed by using a JSPM4210 AFM instrument from JEOL (Japan).

3 Results and discussion

3.1 Bond distances

An important parameter employed in the structural analysis of this type of systems is the molecular separation distance. Due to the large size of both molecules, fullerene and porphyrin, various reference systems can be used to measure this separation. Nevertheless, it is well known that the distance that is used from both theoretical and experimental point of view is always the shortest distance between the two molecules: that is, the porphyrin center and the fullerene point (usually a carbon atom) nearest to the porphyrin molecule.

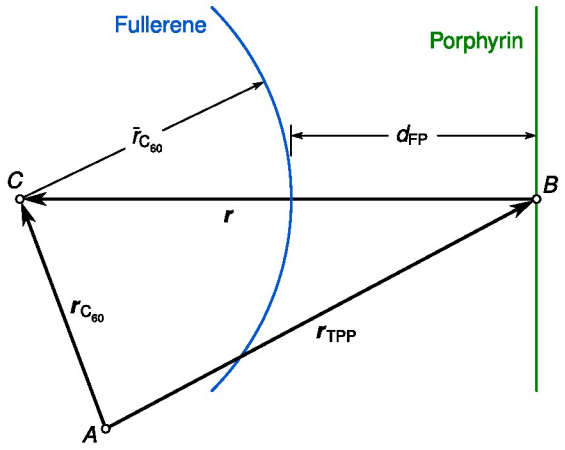

Fig. 2 Geometric parameters of the porphyrin–fullerene system.

However, in the present work, the distance analysis is slightly different from the usual one, since we considered intrinsic geometric and structural regularities that are characteristic of these systems. By using optimized geometry, the position of the mass center for both system were calculated. The mass center of a molecule is calculated as:

$$r_{\text{mc}} = \frac{\sum_i m_i r_i}{\sum_i m_i}, \quad (9)$$

where the i index runs for each nucleus of m mass at the r position in that molecule. From now on, $r_{\text{mc}} = r_{C_{60}}$ will represent the fullerene mass center, and $r_{\text{mc}} = r_{\text{TPP}}$ the porphyrin mass center (Fig. 2). From this representation, we define the distance between both molecules as the magnitude of the vector whose origin is the porphyrin mass center and the end is at the fullerene mass center:

$$d_{\text{cm}} = |r| = \left|r_{C_{60}} - r_{\text{TPP}}\right|. \quad (10)$$

One should note that neither fullerene nor porphyrin molecule (assumed as a disc-shaped with mass center r_{TPP}), exhibit a noticeable deformation. Fullerene molecule can be represented as a sphere of $\bar{r}_{C_{60}}$, where the radii is an average distance between each carbon atom and the mass center.

$$\bar{r}_{C_{60}} = \frac{1}{60}\sum_{i=1}^{60}\left|r_i - r_{C_{60}}\right|. \quad (11)$$

From equations (10) and (11), the shortest distance between fullerene and porphyrin, d_{FP}, is:

$$d_{\text{FP}} = d_{\text{cm}} - \bar{r}_{C_{60}}. \quad (12)$$

To compare our theoretical results to experimental values, we

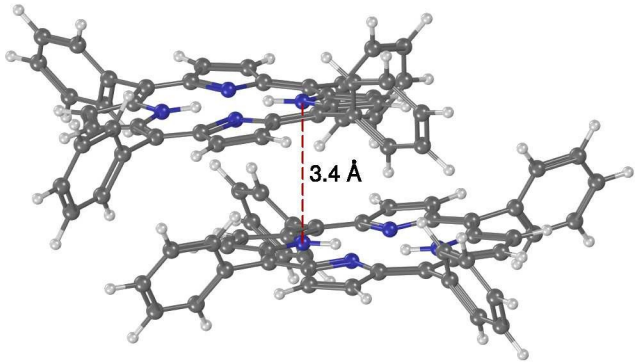

Fig. 3 Optimized geometries of the $H_2TPP\cdots H_2TPP$ dimer, calculated at DFT M05-2X/6-31G(d,p) level of theory.

define the $X_{(\text{exp–theo})}$ term as:

$$X_{(\text{exp–theo})} = X_{(\text{experimental})} - X_{(\text{theoretical})}, \quad (13)$$

where X can be the separation distance (d_{PP} for the porphyrin dimer or d_{FP} for the porphyrin–fullerene complex) or the corrected binding energy (E_{bind}^{CP}) for the corresponding system.

3.2 $H_2TPP\cdots H_2TPP$ dimer

In order to test our computational approaches, we initially performed calculations on the $H_2TPP\cdots H_2TPP$ dimer (Fig. 3). Table 2 shows the distance separations and binding energies (with and without BSSE correction) obtained for the dimer by using the six functionals mentioned above. The theoretical values can be compared to experimental data in the zinc porphyrin–zinc porphyrin system, whose $\pi\cdots\pi$ binding energy is -11.5 ± 2.4 kcal mol^{-1}, and the separation distance between two molecules is 3.4 Å.[40] The separation distances of the dimer (d_{PP}) were obtained as the interplanar distance of separation between both tetraphenylporphines.

As can be seen from Table 2, only the binding energy obtained with B3LYP functional predicts a positive value, the other functionals E_{bind}^{CP} show negative values suggesting formation of the dimer as experimental evidence indicates. The comparison of the separation distances and the binding energy obtained theoretically in this work with those reported by experimental methods

Table 2 Calculated separation distance (d_{PP}, in Å) and binding energies with and without counterpoise (CP) correction for basis set superposition error (E_{bind} and E_{bind}^{CP}, in kcal mol^{-1}) for the $H_2TPP\cdots H_2TPP$ dimer using different DFT functionals and the 6-31G(d,p) set basis.

Functional	d_{PP}(Å)[a]	E_{bind}	δ^{BSSE}	E_{bind}^{CP}
B3LYP	4.7	−3.98	4.72	0.74
CAM-B3LYP	4.3	−7.57	6.56	−1.01
LC-BLYP	3.7	−14.53	9.30	−5.22
B97-D	3.5	−48.62	13.99	−34.62
ωB97X-D	3.5	−48.12	11.83	−36.28
M05-2X	3.6	−19.81	8.46	−11.35
ZnP···ZnP[b]	3.4	−11.5 ±2.4		

[a] d_{PP} is the interplanar distance of separation between both tetraphenylporphines; [b] reported experimental values.[40]

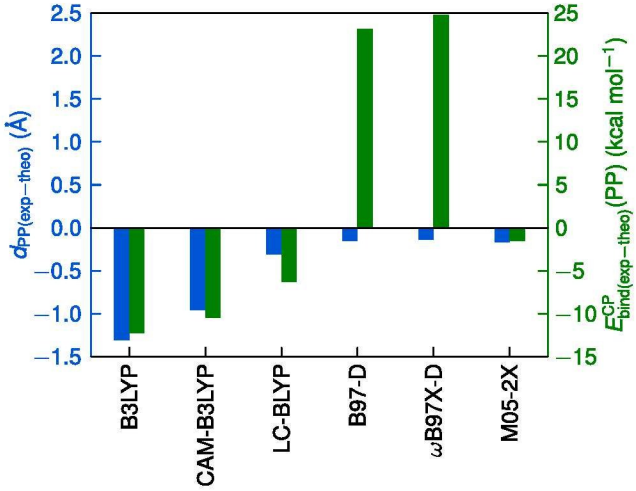

Fig. 4 Comparison of our theoretical results obtained with all functionals to experimental values reported for the $H_2TPP\cdots H_2TPP$ dimer.

was made by using Eq.13, as shown in Figure 4. When the separation distances are compared (blue color in Fig.4), B3LYP and CAM-B3LYP functionals have error bars that are bigger than other functionals; M05-2X, B97-D and ωB97X-D show the most accurate values with small error bars and LC-BLYP functional has intermediate values. Meanwhile, when the binding energy is compared, the error bars (green color in Fig.4) indicate that the B97-D and ωB97X-D functionals overestimate the binding energy by a significant amount of over 20 kcal mol^{-1}, while B3LYP and CAM-B3LYP underestimate this amount by an average value of 10 kcal mol^{-1}. LC-BLYP functional also underestimates the binding energy by a small amount of approximately 6 kcal mol^{-1}. Finally, M05-2X functional shows the smallest error bar among all the functionals used in this work.

From Figure 4, it can be concluded that B3LYP and CAM-B3LYP are the least suitable functionals to study porphyrin dimers, among the others used in this work, because they fail to describe separation distances and binding energy. On the other hand, although B97-D and ωB97X-D functionals give closer separation distances to the experimental ones, they overestimate the binding energy, hence they are not suitable to study porphyrin dimers. We believe that binding energy is overestimated because the use of the empirical dispersion correction (E_{disp}) in Eq.2 is not totally suitable for the $H_2TPP\cdots H_2TPP$ system, which has separation distances that are in a medium-range and not in a long-range where we believe the E_{disp} has a better behavior. LC-BLYP functional is a good option to study porphyrin dimers because of its good description of the exchange interaction to long-distance through the use of the LC method. Finally, according to the small bars in Figure 4 obtained for M05-2X functional, it is possible to conclude that this functional is the one that describes the best the $\pi\cdots\pi$ interaction in the $H_2TPP\cdots H_2TPP$ dimer. The reasons why the M05-2X functional has a good performance will be explained in the next section.

Table 3 Calculated separation distance (d_{FP}, d_{cc} and $d_{C_{60}\cdots N}$, in Å) and binding energies with and without counterpoise (CP) correction for basis set superposition error (E_{bind} and E^{CP}_{bind}, in kcal mol^{-1}) for $H_2TPP\cdots C_{60}$ complex using different DFT functionals and the 6-31G(d,p) set basis.

Functional	d_{FP}	d_{cc}	$d_{C_{60}\cdots N}$	E_{bind}	δ^{BSSE}	E^{CP}_{bind}
B3LYP	3.27	3.37	3.68	−0.89	4.60	2.81
CAM-B3LYP	3.03	3.07	3.37	−4.27	5.79	1.36
LC-BLYP	2.80	2.98	3.19	−8.89	7.28	−2.13
B97-D	2.57	2.65	2.96	−29.03	8.66	−23.32
ωB97X-D	2.65	2.68	3.02	−29.56	7.14	−24.54
M05-2X	2.67	2.86	3.03	−12.91	6.46	−7.66
$H_2TPP\cdot 2\,C_{60}\cdot 3\,C_6H_6$ [a]	2.68 [b]	2.74–2.82 [c]	3.02[c]			

[a] X-ray structure[9]; [b] our calculated values from X-ray structure; [c] reported experimental values[9].

3.3 $H_2TPP\cdots C_{60}$ complex

Table 3 summarizes the separation distances as well as the binding energies calculated with and without BSSE correction (with CP method) for $H_2TPP\cdots C_{60}$ complex, using the six different functionals mentioned previously.

In order to compare our theoretical results to experimental values, the separation distances for $H_2TPP\cdot 2\,C_{60}\cdot 3\,C_6H_6$ X-ray structure[9] are also included in the Table 3. As regards binding energy, the only information derived experimentally (to our knowledge) is the enthalpy values for the separation of fullerenes on tetraphenylporphine-silica stationary phase using different solvents as mobile phases. The values reported are in the range from −1.4 to −2.4 kcal mol^{-1}.[41] In the absence of gas phase experiments, we use the average of this range (−1.9 kcal mol^{-1}) to compare our theoretical calculations. However, due to lack of solvation and temperature effects in our calculations, is expected that the binding energies obtained in this work should have more attractive values (negative values of greater magnitude) than the aforementioned average.

Four different parameters will be used to compare our values with those reported experimentally. The first two, the d_{cc} distance (distance between the geometric center of porphyrin ring and the electron-rich 6:6 bond of pyracylene unit of C_{60}) and the $d_{C_{60}\cdots N}$ distance (the closest contacts of N atoms of tetraphenylporphine with the 6:6 C−C bond) can be compared directly in the Table 3 to the experimental values for the $H_2TPP\cdot 2\,C_{60}\cdot 3\,C_6H_6$ crystal structure. The results from this comparison show that B3LYP and CAM-B3LYP functionals are the ones that fail the most to reproduce these two experimental distances. With B97-D and ωB97X-D functionals, slightly smaller separation distances than the experimental ones are obtained, although similar. The d_{cc} and $d_{C_{60}\cdots N}$ distances obtained from LC-BLYP functional are slightly bigger than the experimental values while with M05-2X functional, almost accurate values are predicted when they are compared to $H_2TPP\cdot 2\,C_{60}\cdot 3\,C_6H_6$ crystal structure. According to these two parameters, the ascending order of accuracy is B3LYP < CAM-B3LYP < LC-BLYP < B97-D < ωB97X-D ≈ M05-2X.

The other two parameter were obtained from Eq. 13 and they were plotted in Figure 5. By comparing the error bars for the $d_{FP(exp-theo)}$ values (blue color in Fig.5), it is obtained that B3LYP and CAM-B3LYP functionals are the ones with the biggest error, while ωB97X-D functional and specially the M05-2X functional have the smallest error bars compared to other functionals used in this work. The B97-D and LC-BLYP functionals have small error bars although not with the same accuracy of M05-2X functional that is the most accurate of the series according to this parameter. Regarding this parameter, the ascending order of accuracy is B3LYP < CAM-B3LYP < LC-BLYP < B97-D < ωB97X-D < M05-2X. On the other hand, when comparing the binding energies (green color in Fig.5), error bars with negative values (repulsive interaction) are obtained for B3LYP and CAM-B3LYP funtionals, whereas the experimental evidence indicates an energetically favored process. Therefore, it is clear that these two functionals are not suitable to describe $TPP\cdots C_{60}$ and related systems. B97-D and ωB97X-D functionals show big error bars with an amount of over 20 kcal mol^{-1} on the positive Y-axis which indicates that binding energy is overestimated. This is similar to the results obtained for the $H_2TPP\cdots H_2TPP$ dimer (Table 2), which suggests that the DFT-D method overestimates the dispersion energy for π···π interactions in both systems. LC-BLYP functional has small error bars, however, it is expected that in gas phase the binding energies should be way over the experimental average value of −1.9 kcal mol^{-1}. M05-2X functional has error bars with a small magnitude of approximately 5 kcal mol^{-1} (positive Y-axis), as it should be expected in the gas phase. These results agree with those obtained for $H_2TPP\cdots H_2TPP$ dimer, where M05-2X also yielded realistic separation distance and binding energy. Regarding this

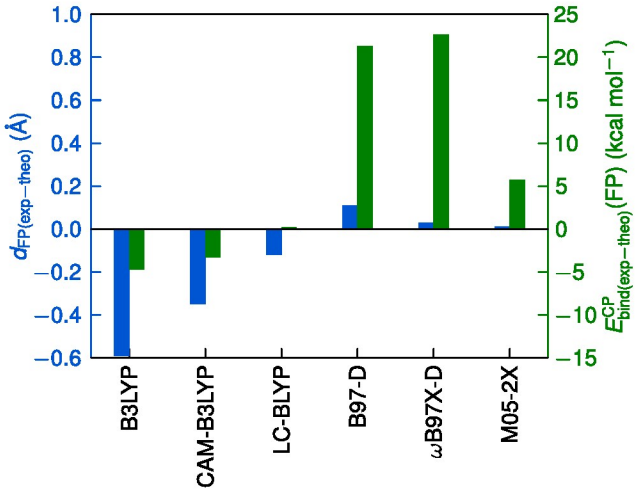

Fig. 5 Comparison of our theoretical results obtained with all functionals to experimental values reported for the $H_2TPP\cdots C_{60}$ complex.

parameter, the ascending order of accuracy is B97-D ≈ ωB97X-D < LC-BLYP < M05-2X.

According to the above analysis, the M05-2X functional is the best to reproduce experimental values for the $H_2TPP\cdots C_{60}$ complex. The ability of the M05-2X functional to reproduce properly experimental values for $H_2TPP\cdots H_2TPP$ and $H_2TPP\cdots C_{60}$ complexes, it is due to several factors, such as, the inclusion of kinetic energy density, its high parameterization for noncovalent interactions, the use of a high percentage of exact exchange of HF (56 %), which allows to describe adequately the exchange interactions to long distances and finally, its good performance to describe dispersion in a medium-range (2–5 Å) as in the case of the systems analyzed in this work. The capacity of the M05-2X functional to describe the dispersion interaction is due to its high parameterization for noncovalent systems, whose separation distances were in a medium-range, and to the nondynamical correlation energy contained in the expression $\left(1-\frac{X}{100}\right)\left(E_X^{\mathrm{DFT}}-E_X^{\mathrm{HF}}\right)$ of Eq.3, that can be explained by the effect of the GGA exchange functionals, as have been reported by other authors.[42,43] In conclusion, although the corrections to dispersion and exchange interaction to medium distances are incorporated in a different way compared to other functionals tested in this report, it is evident from our results that M05-2X functional is the most adequate to describe $TPP\cdots C_{60}$ systems.

Figure 6 shows the curves of the interaction potential energy calculated with BSSE correction for each of the six functionals tested in this work. These curves were obtained by single point energy calculations carried out on equilibrium geometry, by varying the R value within the range of 2.2 to 4.4 Å. The distance d_{FP} was taken as a separation parameter. It is seen that B3LYP and CAM-B3LYP functionals do not predict a stationary point in the potential curve, confirming the conclusion mentioned above that this functionals are not suitable to describe $TPP\cdots C_{60}$ systems. In contrast, B97-D and ωB97X-D show the most attractive interactions, reinforcing the idea that the DFT-D method overestimates the dispersion energy in porphyrin–fullerene complexes, which separation distances are in a medium-range. LC-BLYP calculations predict a curve of potential energy with weaker interactions than the ones obtained with DFT-D and M05-2X functionals. The curve obtained with M05-2X functional occupies an intermediate position among those calculated with LC-BLYP and two DFT-D functionals. As it was mentioned above, M05-2X functional is the most suitable to describe $H_2TPP\cdots C_{60}$ systems, therefore its curve is expected to be the most realistic one from Figure 6.

As anticipated in the introduction, this is the first work where functionals with correction to exchange interaction to long distances with LC method have been used to study $TPP\cdots C_{60}$ systems. This work shows the relevance of this correction to model the porphyrin–fullerene systems correctly. For example, the results obtained with the CAM-B3LYP functional are improved in both separation distances and binding energies regarding the results obtained with B3LYP functional (Table 3). Almost the same happens with the separation distances obtained with the ωB97X-D functional which are more accurate that the ones predicted by B97-D, due to LC method included in the ωB97X-D functional. An even more evident example is that of the energies and separation distances computed with BLYP (in our earlier work[26]) and LC-BLYP functionals (Table 3) are compared. Previously, we obtained separation distances of $d_{cc} = 3.81$ Å and $d_{C_{60}\cdots N} = 4.0$ Å associated with the uncorrected repulsive binding energy of 2.3 kcal mol^{-1} for the same $H_2TPP\cdots C_{60}$ complex by using the BLYP/DNP level of theory,[26] while LC-BLYP calculations give the distances by 0.9 Å closer to the experimental values than the ones obtained with BLYP. Also, LC-BLYP functional predicts uncorrected attractive binding energy ($E_{\mathrm{bind}} = -8,89$ kcal mol^{-1}), which agrees better with the experimental estimates. In conclusion, the correction to long range of exchange interaction is indispensable in order to study $TPP\cdots C_{60}$ systems by DFT.

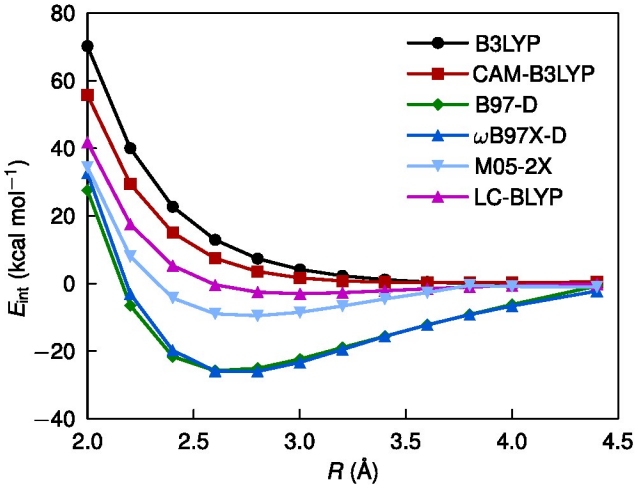

Fig. 6 Calculated intermolecular interaction potentials for the $H_2TPP\cdots C_{60}$ complex with different DFT functionals using the 6-31G(d,p) basis set.

On the other hand, by comparing the binding energy (with CP correction) obtained with LC-BLYP and the one obtained with ωB97X-D functional (Table 3), we can conclude that the energy of dispersion for $H_2TPP\cdots C_{60}$ complex has a magnitude of about 20 kcal mol^{-1}. A similar magnitude for the same system was reported by Liao and collaborators.[27] Although the binding energy and separation distances obtained with B97-D and ωB97X-D by us agree with DFT-D results by others authors,[27–29] in this paper we demonstrate that apparently DFT-D functionals overestimate the dispersion interaction for $TPP\cdots C_{60}$ systems. In addition, as can be seen in Table 3, the δ^{BSSE} values for DFT-D functionals are larger than other functionals used here. Hence, we can conclude that the BSSE correction is especially necessary if a DFT-D functional is used. Finally, from Table 3 it can be seen that the magnitude of δ^{BSSE} is between 4.6 and 8.66 kcal mol^{-1}, whereas the dispersion energy values are about 20 kcal mol^{-1}. In our opinion, it is hardly possible that a fortuitous error cancellation only between BSSE and dispersion energy can lead to good results, as some authors suggested,[27] since both values have different magnitudes.

A detailed comparison of the separation distances and binding energies calculated in this article to other theoretical works can be performed only for B3LYP functional, since the study of $H_2TPP\cdots C_{60}$ complex has not been reported yet with the remain-

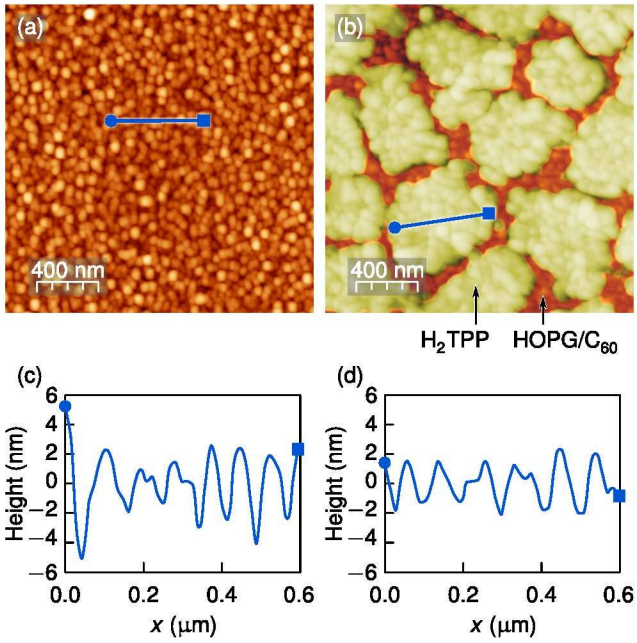

Fig. 7 AFM image (2D view, $2.0 \times 2.0\ \mu m^2$) of (a) C_{60} film on HOPG and (b) H_2TPP film on HOPG/C_{60} deposited by sublimation. AFM height profile of (d) HOPG/C_{60} and (e) HOPG/C_{60}/H_2TPP films.

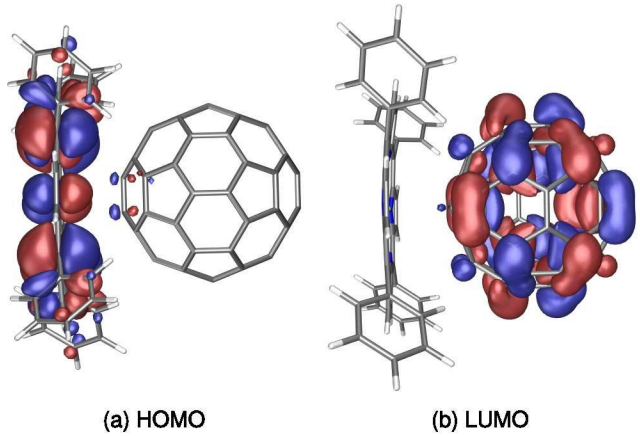

Fig. 8 (a) HOMO and (b) LUMO plots for noncovalent complex $H_2TPP\cdots C_{60}$ obtained with DFT a M05-2X/6-31G(d,p) level of theory.

ing five functionals under discussion. Earlier DFT calculations of $H_2TPP\cdots C_{60}$ complex at the B3LYP/3-21G level of theory[30] produced the intermolecular distance between C_{60} and H_2TPP ring plane of 3.1 Å, as well as an attractive binding energy (without correction to BSSE) of -3.34 kcal mol^{-1}. In the present work, for the same complex we found $d_{cc} = 3.37$ Å value and attractive binding energy of -0.89 kcal mol^{-1}, also without BSSE correction, but with a larger basis set of 6-31G(d,p). On the other hand, our results agree well with another work,[44] where the noncovalent complex of porphine (porphyrin without tetraphenyl substituents) with fullerene was studied by using the B3LYP/6-31G(d) level of theory; the authors reported a separation distance of 3.37 Å, BSSE-uncorrected binding energy of -0.82 kcal mol^{-1}, and corrected (using CP) binding energy of 1.88 kcal mol^{-1}.

When analyzing the binding energies for $H_2TPP\cdots H_2TPP$ dimer (Table 2) and $H_2TPP\cdots C_{60}$ complex (Table 3), it can be seen that the energies for the porphyrin dimer are more negative (attractive) than those obtained for the porphyrin–fullerene dyad. That is, the flat–flat $\pi\cdots\pi$ interaction is stronger than the curved–flat $\pi\cdots\pi$ interaction, in spite of the observation that the separation distances in $H_2TPP\cdots H_2TPP$ dimer are larger than in $H_2TPP\cdots C_{60}$ complex. We attempted to support this result experimentally by using an AFM.

Figure 7(a) shows the morphology of a thin film of C_{60} (thickness about 70 nm according to AFM) deposited by sublimation onto a HOPG support and referred to as HOPG/C_{60}. The film was also used as substrate to grow a thin film of H_2TPP (thickness about 30 nm according to AFM) by sublimation, referred to as HOPG/C_{60}/H_2TPP. According to the AFM height profile (Fig. 7(c) and (d)), the average size of the aggregates is the same in both films, between 50–80 nm. However, roughness average (Ra) is different, 1.54 nm for HOPG/C_{60} film and 0.98 nm for the islands of H_2TPP (green color in Figure 7(b)) in a HOPG/C_{60}/H_2TPP thin film. On the other hand, it was reported that a C_{60} thin film onto graphite has a layer-by-layer growth mode[45]. This contrasts with the result shown in Figure 7(b), where islands of H_2TPP onto HOPG/C_{60} substrate can be clearly distinguished, instead of a homogeneous coverage formed by porphyrin molecules, which indicates a Volmer–Weber (VW) growth mode. This suggests that the adatom–adatom (adatom = H_2TPP in our case) interactions are stronger than those of the adatom-surface (surface = HOPG/C_{60}) interaction. The experimental observation implies that the porphyrin–porphyrin interaction is stronger than the porphyrin–fullerene interaction. This interpretation agrees with the theoretical results shown in Tables 2 and 3, and contradicts the conclusions by Kang and Lin for this and similar systems.[46] Although the AFM experiment refers to the interactions between porphyrin and fullerene at the gas–solid interface, it can useful to compare to the behavior of the $H_2TPP\cdots C_{60}$ system in vacuum.

Finally, Figure 8 shows HOMO and LUMO frontier orbitals generated at the M05-2X/6-31G(d,p) level of theory. As it could be expected, the HOMO is mainly located on porphyrin molecule; at the same time, a minor fraction extends to fullerene cage, thus suggesting an insignificant charge-transfer between the two species. As regards LUMO, it is entirely found on C_{60}.

4 Conclusions

The binding energies and intermolecular distances were calculated for $H_2TPP\cdots C_{60}$ dyad with a series of six DFT functionals; the computed values were compared to experimental and theoretical results previously published. M05-2X functional was found to be the most adequate functional to study $H_2TPP\cdots C_{60}$ and related systems, since it produced most realistic parameters. The ability of M05-2X to represent the electron dispersion energy in the medium distance range of 2–5 Å allows to describe the curved–flat $\pi\cdots\pi$ interactions between porphyrin and fullerene more precisely than other functionals that incorporate DFT-D and LC schemes.

B97-D functional predicted intermolecular distances shorter than those found in experimental X-ray structures and stronger attractive binding energies for $H_2TPP\cdots H_2TPP$ dimer and $H_2TPP\cdots C_{60}$ complex. ωB97X-D functional, which combines DFT-D and LC schemes, showed a good agreement with the experimental intermolecular distances for both systems. However, the binding energies turned to be too negative, apparently since DFT-D scheme overestimates the dispersion energy in both model systems. It has been suggested that the functionals incorporating DFT-D scheme correctly describe the R^{-6} asymptotic distance-dependence of dispersion forces for both medium and long distances.[47] In contrast, meta-hybrid functionals like M05-2X do not include the R^{-6} dependent term, and thus can fail in the studies of noncovalent systems. Nevertheless, in this work we found that in the medium range the dispersion energy for $TPP\cdots C_{60}$ systems is better described with the M05-2X functional, which uses a high parameterization and nondynamical correlation energy, than with DFT-D functionals, that incorporate an empirical dispersion correction.

The use of the LC scheme considerably improves the results for geometry and energy. However, unlike DFT-D and M05-2X functionals, the intermolecular distances obtained with LC-BLYP are slightly larger than the experimental values, and their not very attractive binding energy could not be entirely correct. This is explained by the absence of dispersion correction in the LC scheme.

Finally, our experimental results obtained by means of AFM observations suggest that the porphyrin–porphyrin noncovalent interactions are stronger than the porphyrin–fullerene interactions, despite of that the calculated intermolecular separations show an opposite behavior.

Acknowledgments

Financial support from the National Autonomous University of Mexico (UNAM; grant DGAPA-IN101313) and from the National Council of Science and Technology of Mexico (CONACyT, grant 127299) was greatly appreciated. M. R. and O. A.-S. acknowledge DGAPA-IN106513 and DGTIC UNAM project SC15-1-IR-83. O. A.-S. also thanks DGAPA UNAM for a postdoctoral scholarship CJIC/CTIC/1331/2013.

References

1 (*a*) T. Hasobe, H. Imahori, S. Fukuzumi and P. V. Kamat, *J. Phys. Chem. B*, 2003, **107**, 12105–12112; (*b*) T. Hasobe, H. Imahori, P. V. Kamat and S. Fukuzumi, *J. Am. Chem. Soc.*, 2003, **125**, 14962–14963; (*c*) T. Hasobe, P. V. Kamat, V. Troiani, N. Solladié, T. K. Ahn, S. K. Kim, D. Kim, A. Kongkanand, S. Kuwabata and S. Fukuzumi, *J. Phys. Chem. B*, 2005, **109**, 19–23; (*d*) T. Hasobe, K. Saito, P. V. Kamat, V. Troiani, H. Qiu, N. Solladie, K. S. Kim, J. K. Park, D. Kim, F. D'Souza and S. Fukuzumi, *J. Mater. Chem.*, 2007, **17**, 4160–4170.

2 (*a*) H. Imahori and Y. Sakata, *Eur. J. Org. Chem.*, 1999, **1999**, 2445–2457; (*b*) H. Imahori, *Org. Biomol. Chem.*, 2004, **2**, 1425–1433; (*c*) H. Imahori and T. Umeyama, *J. Phys. Chem. C*, 2009, **113**, 9029–9039; (*d*) H. Imahori, T. Umeyama, K. Kurotobi and Y. Takano, *Chem. Commun.*, 2012, **48**, 4032–4045.

3 H. Zhu, J. Wei, K. Wang and D. Wu, *Sol. Energy Mater. Sol. Cells*, 2009, **93**, 1461–1470.

4 A. Kira, T. Umeyama, Y. Matano, K. Yoshida, S. Isoda, J. K. Park, D. Kim and H. Imahori, *J. Am. Chem. Soc.*, 2009, **131**, 3198–3200.

5 Y. Sun, T. Drovetskaya, R. D. Bolskar, R. Bau, P. D. W. Boyd and C. A. Reed, *J. Org. Chem.*, 1997, **62**, 3642–3649.

6 P. D. W. Boyd, M. C. Hodgson, C. E. F. Rickard, A. G. Oliver, L. Chaker, P. J. Brothers, R. D. Bolskar, F. S. Tham and C. A. Reed, *J. Am. Chem. Soc.*, 1999, **121**, 10487–10495.

7 M. M. Olmstead, D. A. Costa, K. Maitra, B. C. Noll, S. L. Phillips, P. M. Van Calcar and A. L. Balch, *J. Am. Chem. Soc.*, 1999, **121**, 7090–7097.

8 F. D'Souza, G. R. Deviprasad, M. S. Rahman and J. pil Choi, *Inorg. Chem.*, 1999, **38**, 2157–2160.

9 (*a*) D. V. Konarev, I. S. Neretin, Y. L. Slovokhotov, E. I. Yudanova, N. V. Drichko, Y. M. Shul'ga, B. P. Tarasov, L. L. Gumanov, A. S. Batsanov, J. A. K. Howard and R. N. Lyubovskaya, *Chem. Eur. J*, 2001, **7**, 2605–2616; (*b*) D. V. Konarev, A. L. Litvinov, I. S. Neretin, N. V. Drichko, Y. L. Slovokhotov, R. N. Lyubovskaya, J. A. K. Howard and D. S. Yufit, *Cryst. Growth Des.*, 2004, **4**, 643–646.

10 A. L. Litvinov, D. V. Konarev, A. Y. Kovalevsky, I. S. Neretin, P. Coppens and R. N. Lyubovskaya, *Cryst. Growth Des.*, 2005, **5**, 1807–1819.

11 Y. Jung and M. Head-Gordon, *Phys. Chem. Chem. Phys.*, 2006, **8**, 2831–2840.

12 W. Kohn and L. J. Sham, *Phys. Rev.*, 1965, **140**, A1133–A1138.

13 Q. Wu and W. Yang, *J. Chem. Phys.*, 2002, **116**, 515–524.

14 U. Zimmerli, M. Parrinello and P. Koumoutsakos, *J. Chem. Phys.*, 2004, **120**, 2693–2699.

15 S. Grimme, *J. Comput. Chem.*, 2004, **25**, 1463–1473.

16 S. Grimme, *J. Comput. Chem.*, 2006, **27**, 1787–1799.

17 A. Savin and H.-J. Flad, *Int. J. Quantum Chem.*, 1995, **56**, 327–332.

18 H. Iikura, T. Tsuneda, T. Yanai and K. Hirao, *J. Chem. Phys.*, 2001, **115**, 3540–3544.

19 M. Kamiya, T. Tsuneda and K. Hirao, *J. Chem. Phys.*, 2002, **117**, 6010–6015.

20 Y. Tawada, T. Tsuneda, S. Yanagisawa, T. Yanai and K. Hirao, *J. Chem. Phys.*, 2004, **120**, 8425–8433.

21 T. Sato, T. Tsuneda and K. Hirao, *J. Chem. Phys.*, 2007, **126**, 234114–234114–12.

22 Y.-B. Wang and Z. Lin, *J. Am. Chem. Soc.*, 2003, **125**, 6072–6073.

23 Y. Kolokoltsev, O. Amelines-Sarria, T. Y. Gromovoy and V. A. Basiuk, *J. Comput. Theor. Nanosci.*, 2010, **7**, 1095–1103.

24 O. Amelines-Sarria, Y. Kolokoltsev and V. A. Basiuk, *J. Comput. Theor. Nanosci.*, 2010, **7**, 1996–2003.

25 V. A. Basiuk, O. Amelines-Sarria and Y. Kolokoltsev, *J. Comput. Theor. Nanosci.*, 2010, **7**, 2322–2330.

26 V. A. Basiuk, Y. Kolokoltsev and O. Amelines-Sarria, *J. Nanosci. Nanotechnol.*, 2011, **11**, 5519–5525.

27 M.-S. Liao, J. D. Watts and M.-J. Huang, *Phys. Chem. Chem. Phys.*, 2009, **11**, 4365–4374.

28 U. J. Castillo, P. Guadarrama and S. Fomine, *Organic Electronics*, 2013, **14**, 2617–2627.

29 V. A. Basiuk and L. V. Henao-Holguín, *J. Comput. Theor. Nanosci.*, 2014, **11**, 1609–1615.

30 I. Zakharova, O. Kvyatkovskii, E. Donenko and Y. Biryulin, *Phys. Solid State*, 2009, **51**, 1976–1983.

31 S. Boys and F. Bernardi, *Mol. Phys.*, 1970, **19**, 553–566.

32 M. J. Frisch, G. W. Trucks, H. B. Schlegel, G. E. Scuseria, M. A. Robb, J. R. Cheeseman, G. Scalmani, V. Barone, B. Mennucci, G. A. Petersson, H. Nakatsuji, M. Caricato, X. Li, H. P. Hratchian, A. F. Izmaylov, J. Bloino, G. Zheng, J. L. Sonnenberg, M. Hada, M. Ehara, K. Toyota, R. Fukuda, J. Hasegawa, M. Ishida, T. Nakajima, Y. Honda, O. Kitao, H. Nakai, T. Vreven, J. J. A. Montgomery, J. E. Peralta, F. Ogliaro, M. Bearpark, J. J. Heyd, E. Brothers, K. N. Kudin, V. N. Staroverov, R. Kobayashi, J. Normand, K. Raghavachari, A. Rendell, J. C. Burant, S. S. Iyengar, J. Tomasi, M. Cossi, N. Rega, J. M. Millam, M. Klene, J. E. Knox, J. B. Cross, V. Bakken, C. Adamo, J. Jaramillo, R. Gomperts, R. E. Stratmann, O. Yazyev, A. J. Austin, R. Cammi, C. Pomelli, J. W. Ochterski, R. L. Martin, K. Morokuma, V. G. Zakrzewski, G. A. Voth, P. Salvador, J. J. Dannenberg, S. Dapprich, A. D. Daniels, Ö. Farkas, J. B. Foresman, J. V. Ortiz, J. Cioslowski and D. J. Fox, *Gaussian 09 Revision D.01*, Gaussian Inc. Wallingford CT 2009.

33 (*a*) A. D. Becke, *Phys. Rev. A*, 1988, **38**, 3098–3100; (*b*) A. D. Becke, *J. Chem. Phys.*, 1993, **98**, 1372–1377; (*c*) C. Lee, W. Yang and R. G. Parr, *Phys. Rev. B*, 1988, **37**, 785–789.

34 T. Yanai, D. P. Tew and N. C. Handy, *Chem. Phys. Lett.*, 2004, **393**, 51–57.

35 (*a*) J.-D. Chai and M. Head-Gordon, *J. Chem. Phys.*, 2008, **128**, 084106; (*b*) J.-D. Chai and M. Head-Gordon, *Phys. Chem. Chem. Phys.*, 2008, **10**, 6615–6620.

36 Y. Zhao, N. E. Schultz and D. G. Truhlar, *J. Chem. Theory Comput.*, 2006, **2**, 364–382.

37 E. G. Hohenstein, S. T. Chill and C. D. Sherrill, *J. Chem. Theory Comput.*, 2008, **4**, 1996–2000.

38 J. O. Hirschfelder, C. F. Curtiss and R. B. Bird, *Molecular Theory of Gases and Liquids*, John Wiley & Sons, New York, 1954, p. 921.

39 B. Jeziorski, R. Moszynski and K. Szalewicz, *Chem. Rev.*, 1994, **94**, 1887.

40 C. A. Hunter, *Chem. Soc. Rev.*, 1994, **23**, 101–109.

41 J. Xiao and M. E. Meyerhoff, *J. Chromatogr. A*, 1995, **715**, 19–29.

42 N. C. Handy and A. J. Cohen, *Mol. Phys.*, 2001, **99**, 403–412.

43 O. V. Gritsenko, P. R. T. Schipper and E. J. Baerends, *J. Chem. Phys.*, 1997, **107**, 5007–5015.

44 M. J. Shephard and M. N. Paddon-Row, *J. Porphyrins Phthalocyanines*, 2002, **06**, 783–794.

45 D. Kenny and R. Palmer, *Surf. Sci.*, 2000, **447**, 126 – 132.

46 C. Kang and Z. Lin, *J. Theor. Comput. Chem.*, 2006, **05**, 665–684.

47 J. Antony and S. Grimme, *Phys. Chem. Chem. Phys.*, 2006, **8**, 5287–5293.